Efficacy Check of Haralick and Symmetry features for Skin Lesions Classification

Adwait Laud
Department of Computer Engineering
NMIMS University
Maharashtra, India

Shruti Borkar
Department of Computer Engineering
NMIMS University
Maharashtra, India

Shrijanya Rai
Department of Computer Engineering
NMIMS University
Maharashtra, India

Udit Kalra
Department of Computer Engineering
NMIMS University
Maharashtra, India

Dhirendra Mishra
Department of Computer Engineering
NMIMS University
Maharashtra, India

ABSTRACT
Skin cancer is growing on a very fast pace globally. There is a to develop an approach for early detection of skin cancer. Numerous approaches have been used to detect skin lesions using image processing and deep learning techniques. This paper experiments to investigate the results of Machine learning algorithms and ResNet18 Model based on the various inherent features extracted and classify images in the HAMS 10000 database. The accuracy of ResNet18 model on HAMS 10000 dataset is 85 %. The features Correlation, Homogeneity, Energy, Contrast and ASM are extracted from the skin lesions and is classified using Grey Level Co-occurrence Matrices (GLCM) and combined with features asymmetry index, compact index, standard deviation of red, blue and green pixels, lesion-diameter are combined with the features and then are passed to SVM classifier and obtains an average accuracy of 67.5%. Whereas it is found that the combination of SMF features along with Haralick features gives overall best accuracy of 70.2% using Random Forest classifier. Thereby neural networks gives better results than machine learning approaches for lesion classification.

Keywords
GLCM, Skin Cancer, SVM Classifier, ResNet18, Feature extraction

1. INTRODUCTION
The occurrence of harmful ultraviolet (UV) radiation in the earth's atmosphere is consequently increasing due to ozone layer degeneration [1]. Skin cancer is the most common diagnosed cancer worldwide, with one out of every three cancer cases being skin cancer, according to the World Health Organization (WHO). As more solar UV radiation penetrates the atmosphere every year, the number of skin cancer cases continues to grow [2].

Sunlight has an essential role in the development of skin cancer, consequently the chance of developing this type of cancer can be mitigated by protecting the human body from sunlight using several ways [3]. Given the increase in instances, it is critical to have accurate and a variety of cancer testing equipment. The near future could see a revolution in the diagnostic system for skin cancer due to the potential of mobile applications that use machine learning. These apps have the ability to provide low-cost diagnostic care, but it's crucial for general practitioners and dermatologists to receive training on how to use the digital dermoscopy analysis system [2].As a result, several computer support systems are utilized to assist specialists in this field. Machine learning and deep learning are now applied in a various domains other than medicine [3]. Skin lesions' structural abnormalities and color alterations are some distinguishing features for skin cancer classification [3]. Mobile applications have one major limitation, which is the quality of the images produced by these applications. The image quality can be affected by various environmental conditions such as lighting and skin color. Figure 1 provides an example of the skin color images that can be affected by these factors. To address this issue, this study employs the Contrast-Limited Adaptive Histogram Equalization (CLAHE) method as an enhancement technique. This method is utilized to discard inconsistent illumination and increase contrast of the image present in RGB skin images.

2. LITERATURE SURVEY
The previous studies have used bi-directional dermatoscopic feature learning (biDFL) to establish connections between the skin lesions and their relevant contextual information. Previous studies have conducted a comparative analysis of ABCD and three point checklist methods.

The results were used to determine the accuracy of the trained model using a web classifier, and it was inferred that Inception V3 outperformed with accuracy of 72%, while MobileNet V1 classified with an accuracy of 58% [4].

The work is based on the fundamental implementation of ML models by analysing core features that are responsible for influencing the target variable. The research [5] used the MobileNet model and classified with an aggregate accuracy of 83.1%. The model was trained on approximately 12,80,000 images obtained from the 2014 ImageNet challenge and later fine-tuned using 10015 dermoscopy images from the HAMS10000. Another study based on MobileNet implementation done by Sae-Lim [6] after training on the dataset achieved 80.14% accuracy for MobileNet and up to

83.93% accuracy for modified MobileNet. The work is based on the fundamental implementation of ML models by analysing core features that are responsible for influencing the target variable.

3. METHODOLOGY

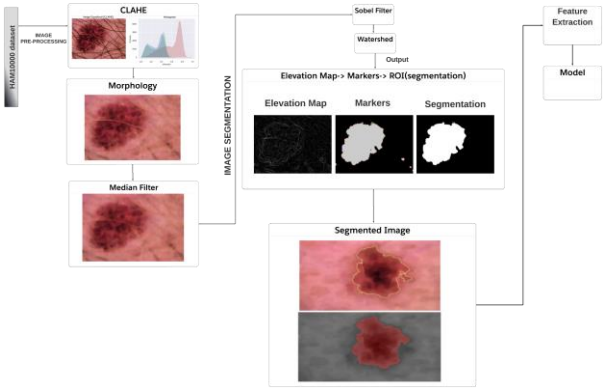

Fig 1: Proposed Model Structure

Figure 1 gives a general overview of the methodology which has been implemented in this research. The data collected from the HAMS10000 dataset is further been preprocessed for which CLAHE has been used, later of the same image morphological closing is done for a better mark of the particular infected area and the last part of the preprocess is using a median filter of the morphed image which was done in the morphology stage. The following stage in the methodology focuses on the image segmentation and feature extraction of the infected area

3.1 Dataset Information

HAMS10000 dataset is a collection of pigmented skin lesions which is used for training and testing proposed models. The dataset focuses on 7 classes of skin lesions. The dataset is diversified on numerous cases of Bowen's disease (akiec), Melanoma and intraepithelial carcinoma etc. which are mentioned below. HAMS10000 dataset is authentic and popular for skin lesion classification. The dataset was released in 2018 and is gathered from multiple sources.

Table 1. Number Of Instances for Each Class

Type of Cancer	No of Instances
Melanocvtic nevi	6705
Melanoma	1113
Benign keratosis-like lesions	1099
Basal cell carcinoma	514
Actinic keratoses	327
Vasucular lesions	142
Dermatofibroma	115

As it is observed in Table 1, Image data for last 4 classes is lower in comparison to other classes, which in turn creates limitations for incisive and precise classification.

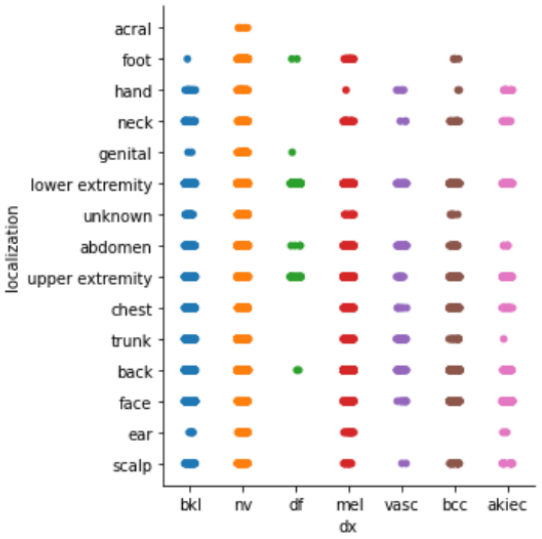

Fig 2: Heading localization of skin cancer

Figure 2 shows the localization of specific skin cancer types and depicts the distribution of the presence of skin lesions across the human body.

3.2 Pre-processing using CLAHE

One of the most common difficulties is the reduction of noise detected in skin cancer. CLAHE [7] is in charge of color enhancement. CLAHE is used in the first stage of pre-processing to reduce noise amplification. Then, to fill cavities or gaps in the foreground object, morphological closure and Median blur are used. Fig 3 shows how the image has been pre-processed using CLAHE, morphological closing and median filter.

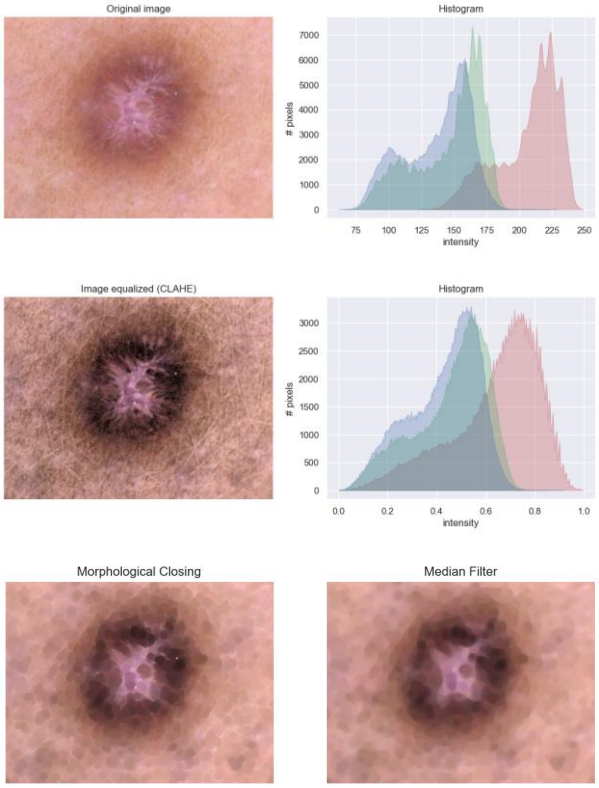

Fig 3: Preprocessing overview

3.2.1 Image segmentation using Watershed

The first step in image segmentation is to convert the image to grayscale. Sobel filter and the ISODATA filter is used to create image markers. The Watershed Algorithm is then implemented to the filtered input to segment it using markers. the attributes of the labelled picture regions are computed and the region containing the lesion if it is at least 1200 px in size is selected [8]. One of the images being segmented using watershed is shown in Fig.4.

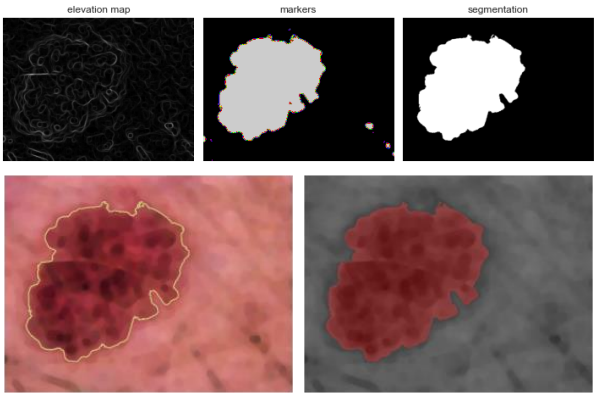

Fig 4: Watershed segmentation

3.2.2 Feature engineering

Feature extraction is a strategy used for dimensionality reduction process, processing techniques helps to divide the raw data and reduce it to more quality rich input for the model. Using feature extraction the best features from the big data set were extracted. Shape, skeleton, texture, and color are derived individually.

The shape is derived from the segmented images, and the skeleton form is created by transforming the segmented images into skeletons. Color features are retrieved from the original image while texture properties are extracted from the texture component. Various combinations of all these features were compared that are developed from a variety of traits and then select the relevant features. In the following section the features are extracted using permutation and combination of various features such as compact index, border irregularity, eccentricity, color variegation, diameter and GLCM feature. There were 60 different feature sets were used for classification. The combinations were made by only taking just the Symmetric features which include asymmetric index, compact index, diameter and eccentricity the next features were selected as the standard deviation of RGB colours and later only the GLCM features were considered. In order to test effectiveness of various features we kept on adding new features sequentially to the feature set used for classification. The features extracted from the image for classification purposes are given below.

3.2.2.1 Asymmetry & Eccentricity:

Asymmetry is derived by division of lesion into 4 sections. The asymmetry involves sector identification by orthogonal axes which passes through the lesion-centroid to derive minimum asymmetry. Figure 5 depicts the image mask, horizontal flip, and difference for asymmetry feature selection.

Asymmetry index= 0.5 * ((diff_horizontal_area / area_total) + (diff_vertical_area / area_total)) (1)

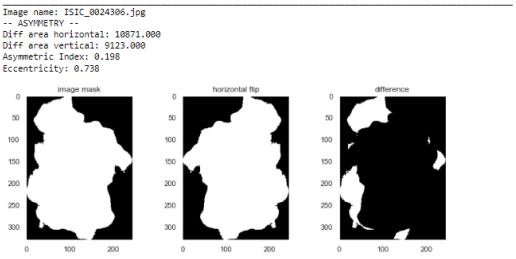

Fig 5. Asymmetry Feature Selection

3.2.2.2 Border irregularity:

Border irregularity refers to an uneven or indistinct edge surrounding a skin lesion. The periphery of the lesion is divided into eight equivalent sections, and if any of these sections have a jagged or abrupt boundary, it is assigned a score of one.

compact_index = (lesion_region.perimeter ** 2) / (4 * pi * area_total) (2)

3.2.2.3 Color variegation:

Color variation is the primary distinguishing factor for melanoma. While the human eye can differentiate between hundreds of thousands of color shades and intensities, it can only distinguish around 100 shades of grey. This means that color can provide a vast amount of supplementary information that simplifies image analysis, including object identification and extraction based on color. A specific color can be described using three independent quantities. Visible colors exist on the electromagnetic spectrum, ranging from 400nm (violet) to 700nm (red). The three deviations are viz;

Red Standard Deviation: StdR,

Blue Standard Deviation: StdB,

Green Standard Deviation: StdG

3.2.2.4 Diameter:

The diameter of a lesion is determined by the major axis length of the optimal-fitted ellipse or longest distance between any two points on the perimeter of the lesion.

3.2.2.5 Texture:

Texture in an image can be identified as spatial variation of pixel brightness intensity. Image processing techniques use a set of metrics to quantify the perceived texture of an image. One such technique is the Grey Level Co-occurrence Matrix (GLCM) algorithm, which is implemented to identify texture of a lesion in medical imaging.

The GLCM algorithm calculates frequency of pairs of pixels with specific intensity values and in a given spatial relationship in an image. Statistical measures are extracted from GLCM matrix to identify texture of the lesion [9].

Feature Vector generated for images include following feature components such as asymmetric index, Eccentricity, Compact index, Standard deviation of Red, Green and Blue image components, Diameter, Correlation, Homogeneity, Energy, Contrast, and Dissimilarity. Formulas for the GLCM features are listed in Table 2.

Table 2. Formula for GLCM features

Features	Formula
Contrast	$f_1 = \sum_{n=0}^{N_\Theta - 1} n^2 \left(\sum_{i=1}^{N_\Theta} \sum_{j=1}^{N_\ominus} p(i,j) \right)$
Correlation	$f_2 = \frac{\sum_i \sum_j (ij) p(i,j) - \mu_x \mu_y}{\sigma_x \sigma_y}$
Dissimilarity	$f_3 = \sum_{i,j=1}^{N} P_{i,j} \lvert i - j \rvert$
Energy	$f_4 = \sum_i \sum_j C^2(i,j)$

4. MODELS IMPLEMENTED:

Multiple combinations of features extracted from the image has been used with various machine learning models to test its accuracy. Various models like K neighbour classifier, Logistic Regression, Decision Tree, Random Forest, Gradient Boost were experimented to check efficacy of features extracted.

However, when there is a lack of data, lower accuracy rates can occur. In such cases, an alternative approach is to implement data augmentation. This strategy artificially increases the amount of training input, which can improve the responsiveness of the network and its ability to anticipate results. This strategy can be especially useful in medical image analysis, where a shortage of data can be a challenge.

As a result, a different approach is considered while implementing ResNet. The second strategy begins with data augmentation.

Data augmentation in figure 6 allows us to artificially increase data in order to make the network more responsive and better at anticipating results.

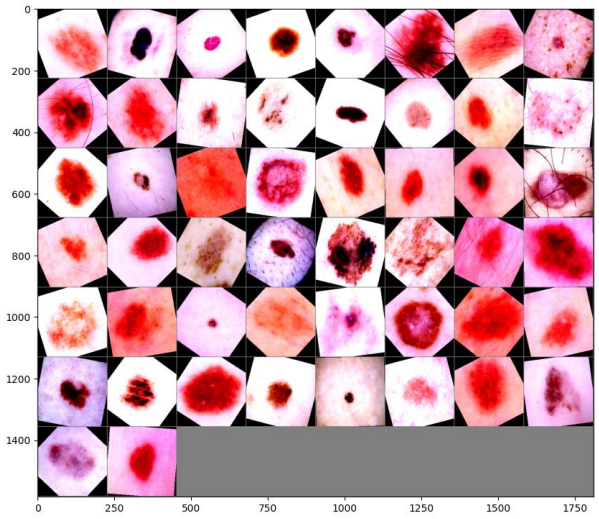

Fig 6. Data Augmentation

5. RESULTS AND DISCUSSION

Following the application of various ML models and the subsequent implementation of Resnet, the following accuracies were predicted by combining various features and obtaining accuracy one by one.

Table 3. Accuracy Table of Combinations with Haralick Features

Method	**Features Selected**				
	SMF + TEXTURE + Correlation	**SMF + TEXTURE +** Correlation + Homogeneity	**SMF + TEXTURE +** Correlation + Homogeneity + Energy	**SMF + TEXTURE +** Homogeneity + ENERGY + Contrast + Correlation	**SMF + TEXTURE +** Correlation Homogeneity + Energy + Contrast + Dissimilarity
KNN	64.7	67.5	66.4	66.5	66.8
Logistic	67.1	67.2	67.6	67.6	67.5
Decision tree classifier	57.8	59.7	60.9	60.6	60.9
Random Forest	69	70.2	69.9	69.9	69.7
Gradient Boost	65	69	69	69	69.2
Ensemble	67	69	69.2	69.2	68.8

Finally, the overall accuracy that is predicted after obtaining the features has been tabulated. Table 3 displays the accuracy of ML models for permutation and combination of features, where SMF denotes symmetric features. To achieve accuracy, SMF and textures were kept constant, and various combinations of GLCM features were used.

Table 4 shows the accuracies using ML models for the permutation and combination of the features where SMF indicates symmetric features. Here, only symmetric features, texture, and GLCM features were taken into consideration. Lastly, Texture and GLCM features were combined together. Table 3 indicates the accuracy when all the features i.e. Symmetric feature, texture and 5 features of GLCM were taken into consideration. The combination of symmetric features and texture features along with Haralick features namely correlation and homogeneity when fed to random forest gives us the highest precision rate i.e. 70.2% and outperforms implementation on previous experimented SVM classifier. Decision Tree classifier gives us 57.8% accuracy which is the lowest in all the experimented cases. The four different category of features extracted from the input images were considered individually for experimentation purpose. This experiment was carried out to understand the effect of individual features on final classification accuracy. These results are presented in Table 4.

Table 4. Accuracy Table of Grouped Features

Method	Features Selected (Accuracy)			
	ONLY SMF	ONLY Texture	ONLY GLCM	TEXTURE and GLCM
KNN	62.1	61.1	63.4	65.0
Logistic	67.2	66.3	67.4	68.1
Decision tree classifier	53.1	53.0	56.4	58.8
Random Forest	66.0	64.7	67.3	68.3
Gradient Boost	66.4	66.7	67.2	68.8
Ensemble	65.6	65.7	66.5	68.1

The best case observed in Table 4 is with Texture and GLCM with gradient boost that is 68.8% which is very close to 70.2% of random forest using SMF and Texture. Inferences indicate that combination of symmetric features (SMF), Texture and specific GLCM features constitute a better precision.

Table 5. Overall Performance Table

Performance	Model							
	SVM Classifier	Logistic Regression	KNN	Decision Tree Classifier	Random Forest	Ensemble	LeNet	ResNet-18
Accuracy	67.5	68.0	66.9	61.9	69.9	69.2	64.0	85.0
Precision	57.3	68.1	66.9	60.8	69.6	60.1	-	-
Recall	67.5	68.1	66.9	60.8	69.6	60.1	-	-
F1 Score	56.6	68.1	66.9	60.8	69.6	60.1	-	-

Table 5 indicates the accuracy, precision, recall and F1-Score obtained when all the features i.e. Symmetric feature, texture and 5 features of GLCM were taken into consideration. Random Forest Classifier gave us the highest performance of 69.9% as compared to other models. Whereas ResNet outperforms all machine learning approaches with Accuracy of 85%.

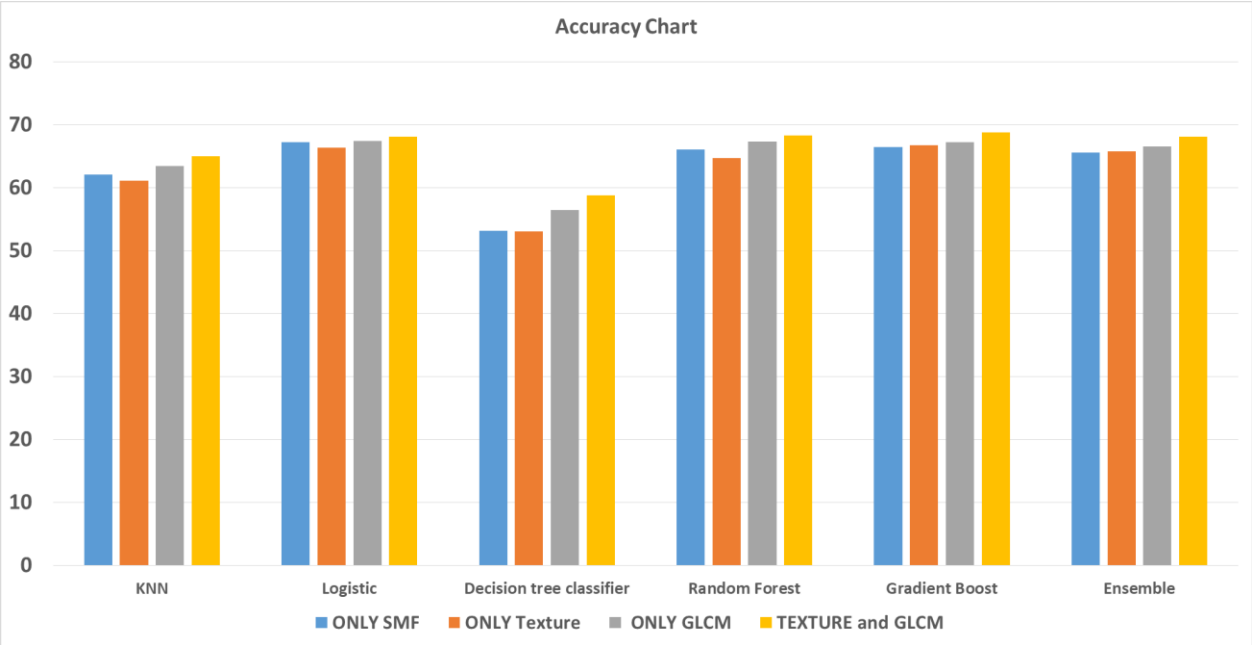

Fig 7. Average Accuracy for specific set of individual features used

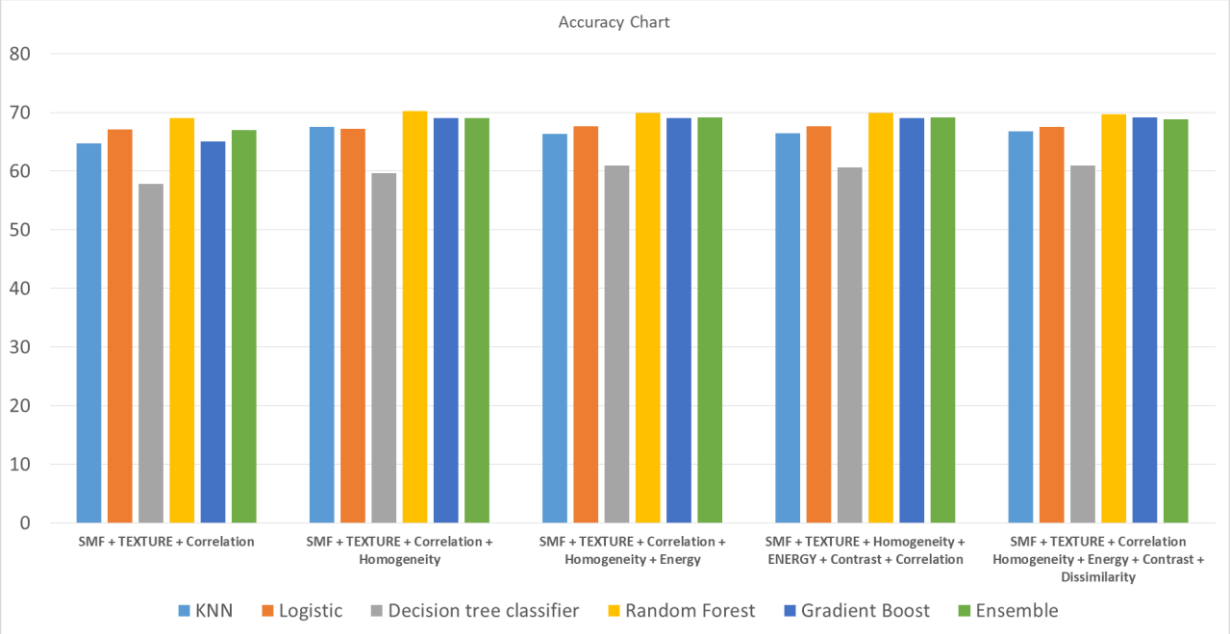

Fig 8. Average Accuracy for specific set of combined features used

Figures 7 and 8 shows average accuracy obtained for experimentations carried out with various combinations of features used for classification in different Machine Learning models. As new features are added, the accuracy of random forest increases linearly. This pattern is consistent with the previous accuracy measures shown in table 4. Random Forest outperforms all other machine learning models after feature extraction, with an accuracy of 69.9%.

This approach also attempts to compare proposed approach with neural network architectures such as given in table 5. The data to Renet-18 model which is used for image classification widely. As per the well known facts the accuracy of neural networks seems to be slightly higher to the ML model with higher computation complexity.

MobileNet, Modified MobileNet, Inception V3, Fix Caps, Sianese Network, ResNet all of these networks have achieved the accuracy in the range of 72% to 92% wherein it is found that the proposed ML model experimentation is close to Inception V3 which is the encouraging result in the area of classification with lesser computation cost.

ResNet-18 gives us accuracy 85%. There are also better options for more accurate and precise results, such as implementing models using a capsule network, which is composed of a collection of neurons, and each neuron's output is composed of a different characteristic of the same feature. This has the advantage of allowing to recognize the entire entity by first recognizing its parts.

The output is input to the next network in the capsule which gives more quality rich analysis for prediction.

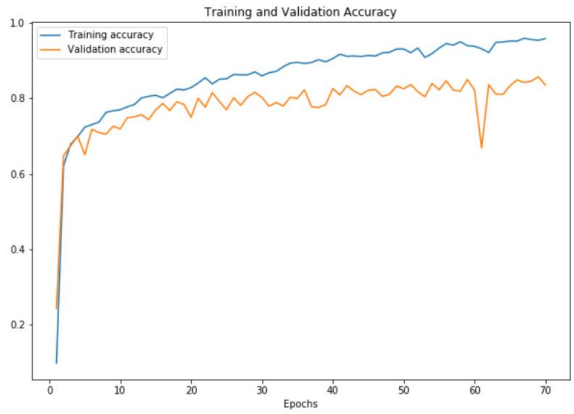

Fig 9: Training and Validation accuracy

Figure 9 represents training and validation accuracy. Y-Axis represents accuracy and X-Axis represents Epochs. The accuracy spikes from 15th epoch and finally at end of 70 epochs we get 85% validation accuracy and training accuracy is higher than 90%

Fig 10: Training and Validation loss

Figure 10 represents training and validation loss. Y-Axis represents Loss and X-Axis represents Epochs.

Table 6. Prediction Accuracy

Skin Cancer Types	Prediction Accuracy	
	Using ResNet	***Using Proposed Model***
Actinic keratosis	66%	47%
Basal cell carcinoma	61%	55%
benign keratosis-like lesions	68%	79%
Dermatofibroma	71%	49%
Melanoma	71%	66%
Melanocytic nevi	93%	95%
Vascular lesions	81%	87%

6. CONCLUSION

Skin cancer types was classified using the extracted features provided as input to various classification models. There were seven distinct classes of skin cancer that had to be predicted using images from dataset.

The dataset used was HAMS10000, which contained 10015 dermatoscopic images, of which 6705 were of cancer type melanocytic nevi skin cancer, 1113 were of melanoma skin cancer, 1099 were of benign keratosis-like lesions, 514 were of basal cell carcinoma, actinic keratoses had 327 images, 142 were of vascular lesions, and 115 were of Dermatofibroma skin cancer.

The proposed solutions used CLAHE algorithm for pre-processing, watershed for algorithm for image segmentation and identified region of interest and the extracted feature set of SMF, Texture, homogeneity and correlation belonging to Haralick feature sets. These features were used with various combinations with machine learning models to classify the images. Average Accuracy calculated for each model and compared with Neural network approaches. These features were combined and permuted one by one to obtain various accuracies. Random forest model implementation along with the feature set combination mentioned above gives the best performance of 70.2% accuracy which is at par with at least with one of the neural networks that is Inception V3 with lower computation cost. The future scope could include implementing a capsule network as a method to achieve more accurate results. Because the input features are a capsule of CNN generated features, the capsule network is more robust than CNN. The ResNet model, which included the combination of all features in one, predicted the highest accuracy.

7. REFERENCES

[1] P. Bumrungkun, K. Chamnongthai and W. Patchoo, "Detection skin cancer using SVM and snake model," 2018 International Workshop on Advanced Image Technology (IWAIT), 2018, pp. 1-4,

[2] A. W. Setiawan, "Effect of Color Enhancement on Early Detection of Skin Cancer using Convolutional Neural Network," 2020 IEEE International Conference on Informatics, IoT, and Enabling Technologies (ICIoT), 2020, pp. 100-103

[3] A. Demir, F. Yilmaz and O. Kose, "Early detection of skin cancer using deep learning architectures: resnet-101 and inception-v3," 2019 Medical Technologies Congress (TIPTEKNO), 2019, pp. 1-4,

[4] K. E. Purnama et al., "Disease Classification based on Dermoscopic Skin Images Using Convolutional Neural Network in Teledermatology System," 2019 International Conference on Computer Engineering, Network, and Intelligent Multimedia (CENIM), 2019, pp. 1-5

[5] Chaturvedi, S.S., Gupta, K., Prasad, P.S. (2021). Skin Lesion Analyser: An Efficient Seven-Way Multi-class Skin Cancer Classification Using MobileNet. In: Hassanien, A., Bhatnagar, R., Darwish, A. (eds) Advanced Machine Learning Technologies and Applications. AMLTA 2020. Advances in Intelligent Systems and Computing, vol 1141. Springer, Singapore.

[6] W. Sae-Lim, W. Wettayaprasit and P. Aiyarak, "Convolutional Neural Networks Using MobileNet for Skin Lesion Classification," 2019 16th International Joint Conference on Computer Science and Software Engineering (JCSSE), Chonburi, Thailand, 2019, pp. 242-24

[7] R. S. M. Alex, S. Deepa and M. H. Supriya, "Underwater image enhancement using CLAHE in a reconfigurable platform," OCEANS 2016 MTS/IEEE Monterey, 2016, pp. 1-5

[8] J. Zhou, Y. Yin and S. Wang, "Image Segmentation Based on Watershed Algorithm," 2021 International Conference on Intelligent Computing, Automation and Applications (ICAA), 2021, pp. 10-13.

[9] R. Maurya, Surya Kant Singh, A. K. Maurya and A. Kumar, "GLCM and Multi Class Support vector machine based automated skin cancer classification," 2014 International Conference on Computing for Sustainable Global Development (INDIACom), 2014, pp. 444-447.

[10] S. S. Teja Gontumukkala, Y. S. Varun Godavarthi, B. R. Ravi Teja Gonugunta, R. Subramani and K. Murali, "Analysis of Image Classification using SVM," 2021 12th International Conference on Computing Communication and Networking Technologies (ICCCNT), 2021, pp. 01-06

[11] Xiaowu Sun, Lizhen Liu, Hanshi Wang, Wei Song and Jingli Lu, "Image classification via support vector machine," 2015 4th International Conference on Computer Science and Network Technology (ICCSNT), 2015, pp. 485-489

[12] Tschandl, Philipp & Rosendahl, Cliff & Kittler, Harald. (2018). The HAM10000 Dataset: A Large Collection of Multi-Source Dermatoscopic Images of Common Pigmented Skin Lesions. Scientific Data. 5. 10.1038/sdata.2018.161.

[13] Fan, Zhu & Xie, Jia-kun & Wang, Zhong-yu & Liu, Pei-Chen & Qu, Shu-jun & Huo, Lei. (2021). Image Classification Method Based on Improved KNN Algorithm. Journal of Physics: Conference Series.

[14] Y. Ibrahim, M. B. Mu'Azu, A. E. Adedokun and Y. A. Sha'Aban, "A performance analysis of logistic regression and support vector machine classifiers for spoof fingerprint detection," 2017 IEEE 3rd International Conference on Electro-Technology for National Development (NIGERCON), 2017, pp. 1-5.

[15] Jijo, Bahzad & Mohsin Abdulazeez, Adnan. (2021). Classification Based on Decision Tree Algorithm for Machine Learning. Journal of Applied Science and Technology Trends. 2. 20-28.

[16] Xu, Baoxun & Ye, Yunming & Nie, Lei. (2012). An improved random forest classifier for image classification. 2012 IEEE International Conference on Information and Automation, ICIA 2012.

[17] Hatefnia, Navid & Ghobad, Marjan. (2018). Radiant Image-Based Data Post-Processing and Simulation. 32. 10.22360/simaud.2018.simaud.032.

[18] H. Song, Y. Zhou, Z. Jiang, X. Guo and Z. Yang, "ResNet with Global and Local Image Features, Stacked Pooling Block, for Semantic Segmentation," 2018 IEEE/CIC International Conference on Communications in China (ICCC), 2018, pp. 79-83

[19] P. S. Karvelis, A. T. Tzallas, D. I. Fotiadis and I. Georgiou, "A Multichannel Watershed-Based Segmentation Method for Multispectral Chromosome Classification," in IEEE Transactions on Medical Imaging, vol. 27, no. 5, pp. 697-708, May 2008, doi: 10.1109/TMI.2008.916962.

[20] K. Haris, S. N. Efstratiadis, N. Maglaveras and A. K. Katsaggelos, "Hybrid image segmentation using watersheds and fast region merging," in IEEE Transactions on Image Processing, vol. 7, no. 12, pp. 1684-1699, Dec. 1998

[21] S. Wang, Y. Yin, D. Wang, Y. Wang and Y. Jin, "Interpretability-Based Multimodal Convolutional Neural Networks for Skin Lesion Diagnosis," in IEEE Transactions on Cybernetics, vol. 52, no. 12, pp. 12623-12637.

[22] L. Wei, K. Ding and H. Hu, "Automatic Skin Cancer Detection in Dermoscopy Images Based on Ensemble Lightweight Deep Learning Network," in IEEE Access, vol. 8, pp. 99633-99647, 2020.

[23] M. A. Anjum, J. Amin, M. Sharif, H. U. Khan, M. S. A. Malik and S. Kadry, "Deep Semantic Segmentation and Multi-Class Skin Lesion Classification Based on Convolutional Neural Network," in IEEE Access, vol. 8, pp. 129668-129678, 2020.

[24] J. -T. Hsu, C. -H. Kuo and D. -W. Chen, "Image Super-Resolution Using Capsule Neural Networks," in IEEE Access, vol. 8, pp. 9751-9759, 2020, doi: 10.1109/ACCESS.2020.2964292.

[25] A. W. Setiawan, T. R. Mengko, O. S. Santoso and A. B. Suksmono, "Color retinal image enhancement using CLAHE," International Conference on ICT for Smart Society, 2013, pp. 1-3, doi: 10.1109/ICTSS.2013.6588092.

[26] J. Zhou, Y. Yin and S. Wang, "Image Segmentation Based on Watershed Algorithm," 2021 International Conference on Intelligent Computing, Automation and Applications (ICAA), 2021, pp. 10-13, doi: 10.1109/ICAA53760.2021.00010.

[27] M. Mishra and M. Srivastava, "A view of Artificial Neural Network," 2014 International Conference on Advances in Engineering & Technology Research (ICAETR - 2014), 2014, pp. 1-3, doi: 10.1109/ICAETR.2014.7012785.

[28] J. Chen, "Image Recognition Technology Based on Neural Network," in IEEE Access, vol. 8, pp. 157161-157167, 2020, doi: 10.1109/ACCESS.2020.3014692.